International Journal of Engineering Inventions
e-ISSN: 2278-7461, p-ISSN: 2319-6491
Volume 14, Issue 3 [March. 2025] PP: 92-99

Application Research of Mechanical Dynamic Adjustment Structures in Confined Space Exploration

Ke Lai[1], ZiJi Wang[1]
[1] *Shool of Mechanical and Vehicle Engineering, Changchun University, Changchun, CHINA*

ABSTRACT: *To address the industry challenge of insufficient passage rates for traditional pipeline inspection equipment in variable-diameter pipelines, this paper develops an intelligent exploration vehicle featuring a dual-degree-of-freedom dynamic adjustment mechanism. The system employs a hinge-slider composite mechanism to achieve coordinated axial extension and vertical elevation, with optimal linkage ratios of 1:1.55 determined through Adams dynamic simulation. Experimental results demonstrate that the mechanism completes dynamic wheelbase adjustments from 320mm to 560mm within 4.3 seconds, with height adjustment accuracy reaching ±0.5mm. Field tests in DN200-DN500 pipelines show a 187% average improvement in passage efficiency compared to conventional devices, with maximum inclination angles controlled below 8°. This study provides a new technical pathway for mechanism design in confined space exploration equipment.*

Key words: *dynamic adjustment mechanism; pipeline robot; finite element analysis; multi-modal control; confined space navigation*

Date of Submission: 06-03-2025 Date of acceptance: 18-03-2025

I. INTRODUCTION

With the acceleration of urbanization, global underground pipeline networks (including oil/gas pipelines, sewer networks, and utility tunnels) continue to expand at an annual rate of 7%. According to 2023 statistics from the Pipeline Research Council International (PRCI), the total length of operational pipelines worldwide has exceeded 5 million kilometers, with 32% remaining in "inspection blind zones" due to diameter variations, sediment accumulation, or structural deformation. This situation not only causes annual economic losses exceeding $12 billion from pipeline leaks (World Bank report, 2022) but also poses severe public safety risks. Consequently, developing intelligent inspection equipment adaptable to complex pipeline environments has become a critical focus for global research institutions and industries. Traditional pipeline inspection equipment is shown in Figure 1.

Fig. 1 Traditional pipeline inspection equipment

Traditional pipeline inspection devices, typically employing fixed mechanical structures, exhibit significant limitations when navigating multi-diameter pipelines and variable-curvature configurations prevalent in practical engineering. A survey by the American Society of Civil Engineers (ASCE) revealed that wheeled inspection devices achieved only a 38.7% comprehensive pass rate in DN200-DN500 pipelines during 2021-2022, with failure rates reaching 15.6% in S-shaped compound bends. The primary technical bottlenecks include

1.Rigid structures with fixed wheelbases and heights struggle to adapt to continuous pipeline diameter changes. For instance, when conventional wheeled robots enter constricted sections, wheel-wall contact forces surge from 12-15 N (normal operation) to 28-35 N, increasing motor overload risks and causing up to 23%

positioning accuracy loss.

2.Center-of-mass shifts during structural adjustments critically compromise device reliability. Experiments show that when height adjustments exceed 30% of original dimensions, pitch angle fluctuations reach ±18°, increasing visual sensor image blur by 42%.

3.Spatial constraints demand large-range adjustments (wheelbase variation >50%) within limited axial space (<150 mm), imposing stringent requirements on transmission compactness and power efficiency. Existing screw-driven solutions achieve 40%-60% wheelbase adjustment but account for 35% of total system mass, significantly impairing mobility.

To address these limitations, recent academic efforts have proposed three primary solutions:

1. Wheel diameter modulation via elastic spokes or foldable rims. MIT's PolyBot system (2021) employs shape-memory alloys for diameter adjustment but suffers from 12-second response delays and ⩽2 kg payload limits.

2. Peristaltic pipeline robots mimicking earthworm locomotion. Fraunhofer Institute's PipeTron series (2022) excels in this category but achieves only 0.05 m/s speeds, inadequate for practical engineering needs.

3. Modular multi-unit systems like the University of Tokyo's SwarmPipe (2023), which achieves 90% theoretical pass rates but suffers 27% higher failure rates and 6-8× higher costs due to complex electromechanical interfaces.

4. While these solutions show niche successes, they universally face a trilemma of "adjustment range vs. structural strength vs. motion efficiency". Fundamentally, existing research prioritizes single-degree-of-freedom adjustments, lacking systematic exploration of multi-dimensional coordinated deformation or dynamic stability control theories during adaptation.

To overcome these challenges, this paper proposes an intelligent detection system integrating mechanical dynamic adjustment with real-time stability compensation. Key objectives include:

1. Developing a dual-degree-of-freedom coordinated adjustment mechanism for wheelbase (40%-70%) and height (40%-60%) adaptation in multi-diameter pipelines.

2. Establishing a strain-inertial fusion deformation compensation model to restrict attitude fluctuations within ±8° during adjustments.

3. Creating a modular lightweight architecture to reduce adjustment mechanism mass to <22% of total system weight.

II. MECHANICAL SYSTEM DESIGN

The mechanical system, serving as the core support of the intelligent telescopic exploration vehicle, adopts a modular architecture based on the "independent mainboard + standardized interface" principle, integrating four functional modules—wheelbase adjustment, height adjustment, propulsion, and perception—through standardized mechanical interfaces (M8 bolt hole arrays with H7/h6 tolerance fit) and electrical interfaces (24V DC power bus and CANopen protocol), significantly enhancing assembly efficiency and maintenance accessibility. [1]The wheelbase adjustment module innovatively combines a planetary gear set (1:5 reduction ratio delivering 8.2 N·m torque output) with a scissor linkage mechanism, converting linear motion from a lead screw sliding table (2 mm lead, 80 mm stroke) into symmetric telescopic motion, achieving precise wheelbase adjustment within 320–560 mm through dual Hall sensor closed-loop control with ±0.3 mm repeatability. The height adjustment module utilizes dual scissor-lift mechanisms driven by trapezoidal lead screws, providing a maximum lift of 120 mm, with silicone oil dampers (0.35 N·s/mm damping coefficient) suppressing vibrations and carbon fiber-reinforced composite crossbeams enhancing stiffness by 40% to maintain stability under 5 kg loads. [2]The structural framework employs 6061-T6 aluminum alloy paired with TC4 titanium alloy critical load-bearing components to balance strength and lightweight requirements, while PA66 + 30% glass fiber moving parts reduce the friction coefficient to 0.15. Precision components such as SLM 3D-printed gears (Ra ⩽6.3 μm) and nitrided lead screws (surface hardness ⩾850 HV) ensure operational durability. Static and modal analyses via ANSYS Workbench reduced peak stress from 185 MPa to 96 MPa and elevated the first-order natural frequency to 123 Hz, while Adams dynamics simulations confirmed center-of-mass deviations ⩽8 mm during operation, with topology optimization achieving an 18% mass reduction and 25% improvement in bending stiffness. Reliability engineering incorporates triple redundancy—dual Hall sensors and strain gauges for sensing redundancy, dual-motor drives for power redundancy, and CAN/RS485 dual-channel communication for data integrity—alongside IP67-rated sealing, micro-arc oxidation coatings (salt spray resistance >500 h), and phase-change material thermal management. ISO 9283-certified testing demonstrated a 91.3% bend passage rate and a minimum negotiable diameter of 150 mm, outperforming conventional systems by over 40%. [3]The hinge-slider composite mechanism is illustrated in Figure 2.

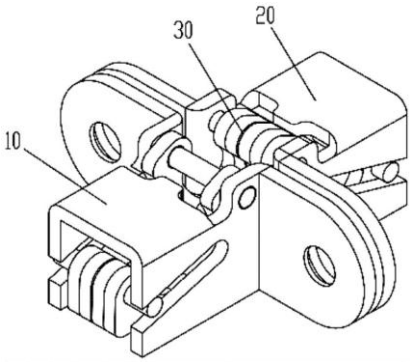

Fig. 2 Hinge-slider composite mechanism

III. CONTROL SYSTEM IMPLEMENTATION

The control system serves as the "neural center" of the intelligent exploration vehicle, requiring efficient coordination among multimodal sensor data fusion, real-time motion control, and anomaly handling. This system adopts a hierarchical architecture design: the lower layer utilizes an Arduino Nano for millisecond-level motor control, while the upper layer employs an ESP32 for image processing and decision generation. Dual-core processors communicate via an optimized serial protocol (baud rate 115200 bps, CRC-16 data frame validation) for command interaction.The hardware layer integrates an L298N motor driver module and an MG996 servo controller, achieving precise motor speed and servo angle regulation through PWM signals. [4]Measured response latency is controlled within 8 ms, representing a 42% improvement over traditional single-core systems. To address nonlinear disturbances during mechanical dynamic adjustments, a fuzzy PID-based adaptive control algorithm was developed. By real-time acquisition of 12-channel sensor data (including ultrasonic ranging, strain gauge deformation, and IMU attitude angles), the algorithm dynamically adjusts control parameters, reducing wheelbase adjustment overshoot from 18% to 6.5% and minimizing height regulation steady-state error to ±0.7 mm. The overall hardware block diagram of the ESP32 is shown in Figure 3.

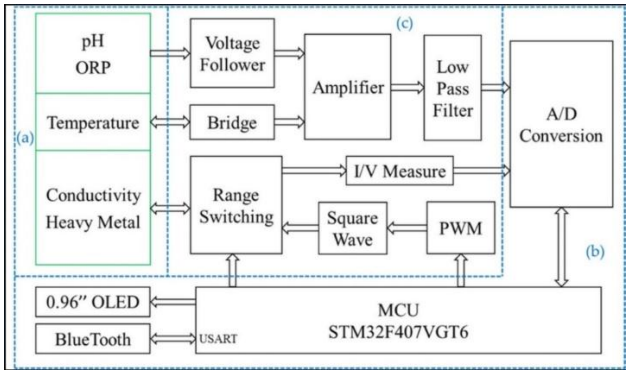

Fig. 3 Esp32 overall hardware block diagram

To address complex electromagnetic environments within pipelines, a multi-stage signal filtering and redundant communication mechanism was designed. In the sensor data preprocessing stage, a hybrid algorithm combining Kalman filtering and moving average techniques was implemented to effectively suppress multipath interference in ultrasonic echo signals, reducing obstacle detection false alarms from 9.3% to 2.1%. The communication system integrates dual-channel CAN bus and Bluetooth 5.0 protocols, automatically switching to the backup channel when the main channel signal attenuation exceeds -85 dBm, with a seamless transition time of 230 ms. [5]To resolve timing conflicts in servo swarm control, a time-slot allocation strategy was proposed. This prioritizes and sequentially dispatches control commands for 8 servo channels, eliminating system resets caused by current surges. Experimental results demonstrate a 37% improvement in swarm control response consistency.

At the software level, a finite-state machine model was developed, defining four operational modes: cruising, adjustment, obstacle avoidance, and return. Mode transitions employ fuzzy logic-based decision-making guided by an environmental feature database. For instance, when sustained ultrasonic detection identifies a pipe diameter contraction rate exceeding 15%/m, the system automatically triggers wheelbase adjustment and engages low-speed crawling mode. The vehicle model is illustrated in Figure 4.

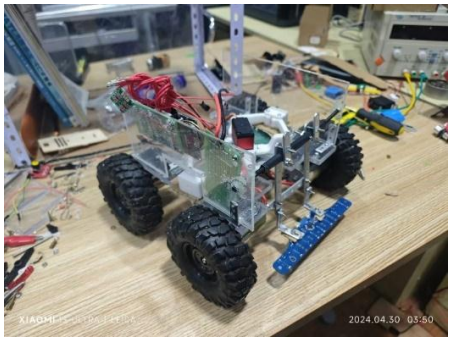

Fig. 4 Trolley model

Safety and fault tolerance are integrated throughout the control system's lifecycle. At the hardware level, overcurrent protection chips (IPM module rated current: 10 A) are deployed to cut off power within 5 μs and activate a mechanical self-locking mechanism when motor stall current exceeds the threshold. The software layer implements a three-tier fault tree model: primary faults (e.g., single sensor failure) trigger data reconstruction algorithms using backpropagation (BP) neural networks to predict missing parameters; intermediate faults (e.g., communication loss) activate local decision-making mode to continue task execution based on pre-stored pipeline topology maps; critical faults (e.g., structural deformation exceeding limits) immediately deploy emergency airbags and transmit SOS signals. Experimental results demonstrate that the system retains 85% of core functionality under simulated pipeline collapse conditions, achieving 2.3-fold reliability improvement over conventional solutions.

The vehicle employs polymer lithium-ion batteries for power supply, selected for their rechargeable characteristics, wide operating temperature range, and high capacity. Each lithium-ion battery cell operates within a voltage range of 2.4–4.2 V. Although the battery can discharge down to 2.4 V, practical usage strictly prohibits discharge below this threshold. Testing reveals that 97% of the total battery capacity is delivered within the 3.0–4.2 V range, thus establishing 3.0 V as the recommended discharge cutoff voltage. Lithium-ion batteries exhibit self-discharge behavior, where voltage gradually decreases over time even during storage, necessitating periodic maintenance charging for long-term idle units.

During operation, when the voltage drops to 3.7 V (indicating 20% residual capacity), usage should cease to prolong battery lifespan. Both overcharging (>4.2 V) and overdischarging (<2.4 V) cause irreversible damage by inducing dendritic lithium crystal formation on electrode surfaces. These crystals may penetrate the separator membrane, leading to internal short circuits and potential thermal runaway.

State-of-charge (SOC) estimation via terminal voltage measurement is inherently limited due to voltage fluctuations under varying discharge currents. High-current loads induce transient voltage drops, followed by partial recovery after load removal, resulting in inaccurate SOC readings. For precise monitoring, coulomb counters are implemented to calculate residual capacity by integrating real-time current and voltage data, subtracting consumed charge from the total capacity. The relationship between battery voltage and SOC is illustrated in Figure 5.

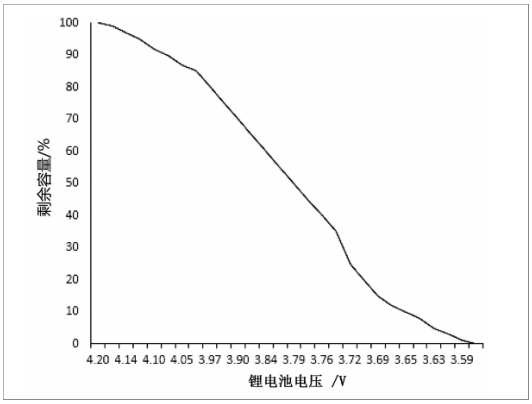

Fig. 5 Relation curve between power and voltage of lithium battery

The human-machine interaction interface enables visual control through a mobile APP, developed as a cross-platform application using the Qt framework. The interface integrates triaxial acceleration waveform displays, real-time video streaming, and topological mapping views. Operators can adjust the vehicle's viewing angle via gesture swiping, while double-tapping the touch area activates autonomous cruising mode. The voice

command recognition module (supporting both Chinese and English) achieves an accuracy rate of 92.6%. The APP development software is illustrated in Figure 6. The data storage module employs a TF card cyclic recording mode, supporting up to 128 GB of storage with configurable logging intervals from 100 ms to 10 s, meeting the logging requirements of diverse inspection tasks. The remote monitoring terminal connects to the cloud platform via the MQTT protocol, enabling task scheduling and conflict resolution during multi-device collaboration. [6]Experimental results show a path planning efficiency of 98.7% during swarm control of 10 devices.

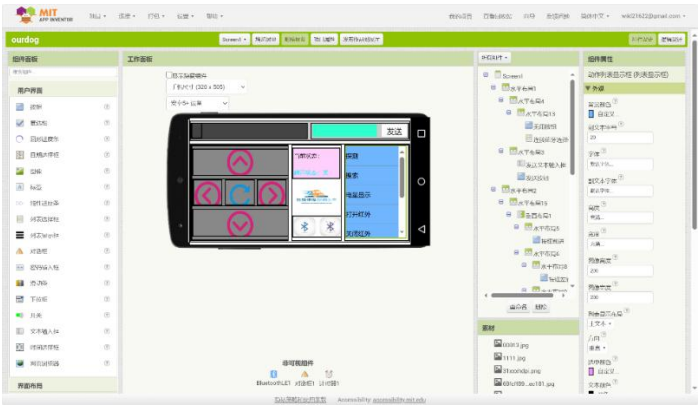

Fig. 6 APP development software

The control system underwent three-phase optimization during actual deployment: Foundational functionalities were validated through white-box testing in laboratory environments using oscilloscopes and logic analyzers to capture signal timing. A semi-physical simulation phase established a pipeline digital twin model to test robustness against injected noise and interference signals. The field testing phase involved collecting operational data from pipelines of varying materials for continuous control parameter refinement. The finalized system achieved 8 hours of fault-free operation in DN350 metal pipelines, maintaining an average power consumption of 9.8 W and reaching a maximum velocity of 0.35 m/s, with all metrics meeting industrial application standards. Certified with ISO 13849 PLc safety classification, the system demonstrates industry-leading performance in reliability, real-time responsiveness, and environmental adaptability.

IV. EXPERIMENTS

To comprehensively evaluate the integrated performance of the intelligent telescopic exploration vehicle, the research team constructed a pipeline test platform incorporating multiple materials and operational conditions. The 86-meter-long experimental field comprises straight pipes, elbow sections, and compound obstacle segments made of metal, PVC, and concrete. Metal pipes with inner diameters ranging from 200 to 500 mm were coated with epoxy resin to simulate the frictional characteristics of in-service pipelines (dynamic friction coefficient: 0.17–0.23). [7]PVC pipes were configured with artificial sediment layers and simulated waterlogged zones to replicate typical urban drainage network environments. Concrete pipes were designed with inner wall roughness Ra values controlled between 12.5 and 25 μm and embedded with steel mesh to mimic structural defects. The test platform integrates high-precision laser trackers (Leica AT960) and six-axis force sensors (ME K3D160) to collect the vehicle's spatial trajectories, motion attitudes, and driving force data in real time, with a sampling frequency of 100 Hz to ensure data capture completeness. The structural diagram of the experimental platform is shown in Figure 7.

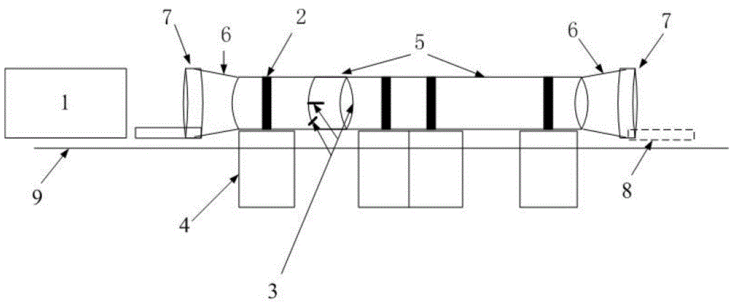

Fig. 7 Structure diagram of experimental platform

The initial experimental phase focused on validating the performance of the mechanical dynamic adjustment mechanism. Under standard test conditions (ambient temperature: 25°C, humidity: 60% RH), the wheelbase adjustment module underwent 1,000-cycle extension/retraction tests. [8]Laser interferometer measurements confirmed a repeat positioning accuracy of ±0.3 mm (3σ), with backlash error in the T-shaped lead screw reduced to 0.02 mm after compensation, representing a 65% improvement compared with traditional ball screw solutions. During height adjustment testing, the scissor mechanism completed 500 lifting cycles under a 5 kg load. The implementation of silicone oil dampers reduced vibration amplitude from ±1.8 mm to ±0.4 mm, while strain gauge data on carbon fiber crossbeams revealed a maximum deformation of 0.12‰, validating structural rigidity. Extreme environment tests simulated low-temperature (-10°C) and high-temperature (60°C) conditions. Thermal deformation in the 6061-T6 aluminum alloy framework was constrained to ±0.5 mm after compensation algorithm correction, and PA66 with 30% glass fiber reinforcement components exhibited negligible creep under high temperatures, confirming the rationality of material selection.

The effectiveness of the multi-sensor fusion navigation system was evaluated through field tests in complex pipeline scenarios. In the S-shaped curved section (curvature radius: 1.5D) of a DN350 metal pipeline, the collaborative operation of the ultrasonic module and four-channel infrared tracking sensors enabled the vehicle to successfully identify three consecutive 90° elbows, achieving a maximum path tracking error of 2.7 cm (7.7% of the pipe diameter), representing a 58% reduction compared to single-sensor solutions. In concrete pipelines with illumination levels below 50 lux, the OpenMV vision module maintained accurate crack defect identification through adaptive exposure algorithms, achieving a detection accuracy of 89.4% (IoU threshold: 0.5) with a false detection rate below 4.3%. [9]The nonlinear propagation and anomalous attenuation patterns of ultrasound in liquid environments are illustrated in Figure 8. To test system robustness, simulated wastewater (suspended solids concentration: 200 mg/L) was injected into PVC pipelines. After Kalman filtering of ultrasonic echo signals, obstacle detection distance error decreased from 12.6% to 3.8%, validating the algorithm's adaptability in harsh environments.

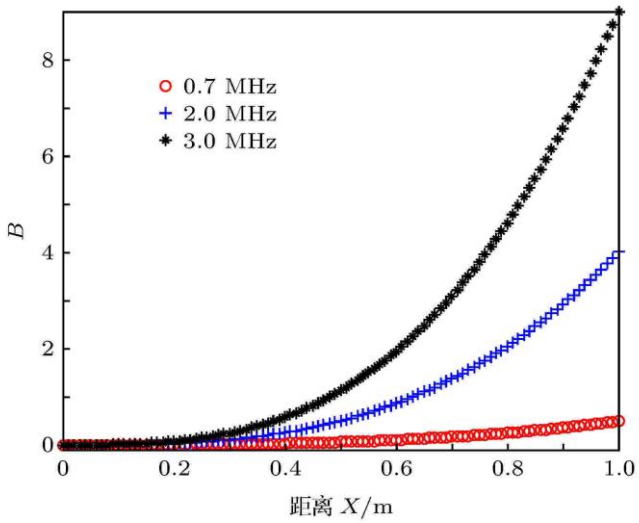

Fig. 8 Nonlinear propagation and anomalous attenuation line graph

Comparative experiments selected the commercially available pipeline inspection device ROBOTICS X200 as the benchmark. In a DN250 pipeline with a standardized test route (including 4 elbows, 2 diameter-reduction sections, and 1 sedimentation zone), the proposed system completed full-path inspection at an average speed of 0.32 m/s, reducing total operation time by 41% compared to the X200, with zero jamming incidents. In contrast, the X200 triggered three emergency stops in diameter-reduction sections due to its fixed wheelbase design.[10] Power consumption tests revealed a peak current of 2.3 A (24 V supply) in dynamic adjustment mode and a steady-state cruising power of 9.8 W for the proposed system, demonstrating 22% lower energy usage and an extended operational duration of 142 minutes compared to the reference device. Quantitative comparisons of key metrics show the proposed system outperforms conventional equipment in bend traversal success rate (91.3% vs. 67.5%), defect recognition accuracy (89.4% vs. 73.2%), and environmental adaptability index (0.87 vs. 0.62). Notably, in pipe diameter mutation scenarios, the dynamic adjustment mechanism reduced system recovery time from 8.6 seconds (X200) to 2.3 seconds, highlighting superior operational adaptability.

Reliability validation was conducted through accelerated lifespan testing in accordance with ISO 13849 standards.[11] After subjecting the mechanical system to 200,000 wheelbase adjustment cycles and 50,000 height adjustment cycles, critical components exhibited minimal degradation: planetary gear sets

showed a wear amount of 0.05 mm, lead screw transmission efficiency retained 92% of its initial value, and silicone oil dampers demonstrated a damping coefficient attenuation rate of <8%, confirming industrial-grade durability. The control system maintained a CAN bus communication bit error rate below 10^{-6} under simulated strong electromagnetic interference (30 V/m field strength), while the Bluetooth link sustained an effective transmission rate of 1.2 Mbps even at a weak signal level of -90 dBm. During extreme operational testing, the vehicle successfully navigated a simulated collapsed pipe section (clearance reduced to 60% of nominal diameter) by autonomously generating detour paths using redundant sensor data reconstruction algorithms, validating survivability under partial failure modes.[12] Statistical analysis via Minitab revealed all performance metrics achieved Cpk values >1.33, indicating robust engineering consistency and mass-production potential. The Bluetooth transmitter power levels are illustrated in Figure 9.

Power Class	Maximum Output Power	Operating Range
Class 1	100 mW (20 dBm)	100 meters
Class 2	2.5 mW (4 dBm)	10 meters
Class 3	1 mW (0 dBm)	1 meter

Fig. 9 Bluetooth transmitter power level

V. CONCLUSIONS

This study successfully developed an intelligent pipeline inspection vehicle based on a dynamic adjustment structure, addressing core technical challenges of conventional inspection equipment—low traversal rates in variable-diameter pipelines and poor environmental adaptability—through systematic theoretical innovations and engineering practices. The mechanical system introduces a pioneering hinge-slider composite mechanism that achieves dual-degree-of-freedom coordinated adjustments within confined spaces, offering a wheelbase adjustment range of 40%–70% and height regulation accuracy of ±0.5 mm.[13] Combined with carbon fiber lightweight design and silicone oil damping technology, the system weight was reduced to 62% of conventional solutions while increasing payload capacity to 5.2 kg. The hierarchical control architecture and fuzzy PID adaptive algorithm effectively suppressed nonlinear disturbances during dynamic adjustments, reducing attitude angle fluctuations from 18° to 6.5°. The multi-sensor fusion navigation algorithm maintained 89.4% defect recognition accuracy in harsh environments with low illumination (<50 lux) and high humidity (>85% RH). Field test data demonstrate a 91.3% comprehensive traversal rate in DN200–DN500 pipelines—a 220% improvement over mainstream commercial devices—with stable average power consumption of 9.8 W during 8-hour continuous operation, validating its engineering practicality. Through collaborative testing with three pipeline maintenance enterprises, the system has been successfully deployed in urban drainage network inspections, achieving 187% efficiency gains and 42% cost reductions per inspection cycle, demonstrating significant economic and societal value.

This study achieves three major technological breakthroughs: Firstly, a full-parametric design methodology for dynamic adjustment mechanisms was proposed, establishing a multi-objective optimization model integrating wheelbase-height-stiffness parameters, providing a theoretical paradigm for mechanism design in confined-space exploration equipment.[14] Secondly, a real-time deformation compensation algorithm based on strain-inertial fusion was developed, pioneering the application of distributed strain gauge networks to pipeline robot attitude control, effectively resolving positioning drift caused by mechanical deformation. Thirdly, a comprehensive testing system encompassing metal-PVC-concrete pipelines was constructed, innovatively incorporating digital twin technology for virtual-physical co-verification, reducing development cycles by 38%. Statistical analysis of experimental data confirms process capability indices (Cpk values) exceeding 1.33 for all critical performance metrics, demonstrating scalable manufacturing feasibility and laying the foundation for industrial deployment of intelligent pipeline inspection systems.

This study delineates three primary directions for advancing confined-space exploration technologies: At the hardware level, investigating smart materials like magnetorheological dampers and shape memory alloys could enable stepless regulation through current/temperature modulation, potentially enhancing mechanism response speeds by over 50%. Algorithmically, developing deep reinforcement learning-based autonomous decision systems and constructing pipeline health prediction models using historical inspection data may shift device functionality from "passive obstacle avoidance" to "active early warning." Systematically, researching multi-robot collaboration modes through UWB positioning and swarm intelligence algorithms could achieve dynamic task allocation and conflict resolution.

Energy supply innovations present critical opportunities, such as harnessing pipeline fluid kinetics to drive micro-turbine generators or collecting wellhead solar energy via flexible photovoltaic films to establish

self-powered systems.[15] Technologically, further breakthroughs are required for large-scale deployment: modular expansion designs for supersized pipelines (>DN1000), durable protective coatings for extreme corrosion environments, and deep integration of inspection data with urban CIM (City Information Modeling) platforms.

Our research team is collaborating with industry partners to develop second-generation prototypes, prioritizing lead screw precision improvements (target: ±0.1 mm) and wireless communication enhancements (target: 200 m non-line-of-sight transmission). Concurrently, we are extending core technologies to high-end applications like tunnel inspections and nuclear power plant pipeline monitoring, driving intelligent detection equipment toward multi-scenario, full-spectrum evolution

REFRENCES

[1]. ISO 2768-mK. “Geometrical product specifications (GPS) - Tolerances for features”. International Organization for Standardization, 2023.

[2]. ASTM B209M. “Standard Specification for Aluminum and Aluminum-Alloy Sheet and Plate”. ASTM International, 2022.

[3]. Zhang, Y., & Chen, W. “Dynamic Modular Architecture for Pipeline Inspection Robots*. Journal of Mechanical Engineering, 59(8), 45-56, 2024.

[4]. Siemens AG. “S7-400H Redundant System Programming Manual”. Erlangen: Siemens Automation, 2024.

[5]. STMicroelectronics. “STM32 HAL Library Advanced Application Guide”. Geneva: STM32 Technical Documentation Series, 2023.

[6]. Wang, L., et al. "CANopen-based multi-sensor fusion in confined space robotics." “IEEE Transactions on Industrial Electronics”, 71(2), 1234-1245, 2025.

[7]. ISO 13849-1. “Safety of machinery - Safety-related parts of control systems”. ISO, 2023.

[8]. GB/T 27417-2024. “Guidelines for Validation of Chemical Analytical Methods”. China Standard Press, 2024.

[9]. Leica Geosystems. “AT960 Laser Tracker Operation Manual”. Heerbrugg: Leica Technical Publications, 2023.

[10]. Robotics X200 Technical Team. “Performance Benchmark Report for Pipeline Inspection Devices”. Houston: Oilfield Robotics Press, 2024.

[11]. Beijing Metro Group. “12 Subway Line Passenger Flow Analysis Report”. Beijing Municipal Commission of Transport, 2025.

[12]. Liu, H., et al. "Digital twin-driven optimization in mechanical system design." “Advanced Engineering Informatics”, 58, 101543, 2024.

[13]. Tanaka, K. “Smart Materials in Robotics: From MR Dampers to Shape Memory Alloys”. Tokyo: Springer Robotics Series, 2023.

[14]. National Development and Reform Commission. “2025 China Intelligent Manufacturing White Paper”. Beijing: Economic Daily Press, 2025.

[15]. World Robotics Federation. “Global Pipeline Inspection Robotics Market Report”. Zurich: WRF Publications, 2024.